Mass Spectrometric Analysis of Nitrogen- and Phosphorus-Containing Pesticides by Liquid Chromatography–Mass Spectrometry

Dietrich Volmer and Karsten Levsen

Department of Analytical Chemistry, Fraunhofer Institute of Toxicology and Aerosol Research, Hannover, Germany

A series of nitrogen- and phosphorus-containing pesticides (amines, anilides, carbamates, phosphonates, phenylureas, sulfonylureas, and triazines) was examined by thermospray (TSP) ionization. A method is described that employs off-line and on-line solid-phase extraction and TSP liquid chromatography–mass spectrometry (LC-MS) with time-scheduled selected ion monitoring (SIM) for environmental monitoring of these pesticides in aqueous samples. SIM detection limits for the pesticides analyzed in conjunction with reversed-phase high-performance liquid chromatography range from 40 to 600 pg. In addition, methods for inducing fragmentation in thermospray LC-MS are presented. The structural information gained therefrom can be used to confirm a tentative identification. Therefore, fragmentation pathways under certain experimental conditions were investigated. Atmospheric pressure chemical ionization, electrospray, fast-atom bombardment, ^{252}Cf plasma desorption, and collision-activated dissociation spectra are presented for several pesticides to confirm the proposed pathways and to gain additional and complementary information. Further confirmation may be achieved by postcolumn addition of different alkylated amines to the carrier stream in the TSP operation to induce postcolumn on-line derivatization (POD) reactions in the condensed phase of the vaporizer probe with selected pesticides. Additional clustering reactions in combination with solvent-mediated chemical ionization are observed by the POD technique. Both processes can be used to enhance the structural information from TSP spectra and thus the specificity of the method. *(J Am Soc Mass Spectrom 1994, 5, 655–675)*

The National Survey of Pesticides in Ground Water [1] published by the U.S. Environmental Protection Agency (EPA) lists 126 polar compounds as potential groundwater contaminants. Although the EPA does not prescribe limit values for these compounds, the Commission of the European Communities (CEC) [2] has set maximum admissible concentrations for pesticides in drinking water (100 ng L^{-1} of an individual pesticide and 500 ng L^{-1} for the sum of all pesticides). For the verification of these limits, universal methods are required that allow the determination of as many as possible of the relevant agents, preferably within one common method.

Gas chromatography (GC) is the traditional method for the analysis of pesticides. The widespread use of GC mass spectrometry is due to the existence of reliable, specific, and sensitive methods for analyzing hundreds of organic compounds including many pesticides in several matrices. However, pesticides amenable to GC are restricted to those with low polarity and sufficient volatility. Several techniques are available to convert at least a limited number of nonvolatile compounds to derivatives amenable to GC. Searching for new derivatization procedures is not attractive because these methods are time-consuming and rarely can be incorporated into a universal method for a wide variety of pesticides from different compound classes.

Method development becomes more difficult if the analysis is extended to metabolites and other degradation products of pesticides. These compounds are often very polar. Thus even if the original pesticides can be analyzed by GC, the method often fails when applied to degradation products. Furthermore, the polar nature of most pesticides and their partial high water solubility explains why these compounds represent potential water pollutants. For such polar pesticides, liquid chromatographic methods can be applied successfully. Conventional detectors, such as UV or photodiode array detectors (DAD), can be used for an unambiguous identification of pesticides in environmental samples for certain compound classes, for example, nitrophenols [3]. Furthermore, *N*-methylcarbamates can be

Address reprint requests to Dietrich Volmer, Fraunhofer Institute of Toxicology and Aerosol Research, Nikolai-Fuchs-Strasse 1, D-30625 Hannover, Germany.

1044–0305/94/$7.00

Received October 11, 1993
Revised February 2, 1994
Accepted February 17, 1994

analyzed by means of a specific postcolumn reaction system using a fluorescence detector [4]. However, in most instances these detectors do not provide sufficient structural information for metabolism studies, nontarget analysis, or even target analysis in environmental samples because the UV spectra of a given pesticide compound class are often almost identical, and differences between compound classes are frequently small. Furthermore, several pesticides have a low UV absorbance because they lack a strong chromophore. Hence a UV or DAD detector is not universally applicable. However, combined liquid chromatography–mass spectrometry (LC-MS) has demonstrated its potential for analyzing a broad spectrum of pesticides, including both typical "GC pesticides" and "high-performance liquid chromatography pesticides" [5, 6].

Nowadays, thermospray (TSP) [5–15], particle-beam (PB) [16], and, more recently, electrospray (ESI) and atmospheric pressure chemical ionization (APCI) [17, 18] are the most commonly used LC-MS interfaces for target and nontarget analysis of pesticides from various matrices. At present, TSP is most widely used because of its sensitivity as compared to PB and its compatibility with conventional high-performance liquid chromatography (HPLC) systems as compared to ESI. The lack of structural information obtained from TSP mass spectra can readily be overcome, for example, by variation of the gas-phase and vaporizer temperature to induce controlled chemical reactions during TSP vaporization and ionization [7], the use of external ionization media and tandem mass spectrometry techniques [19], repeller-induced fragmentation [20], additional cluster ions formed with solvent or additive molecules, and by using the complementary information of positive and negative ion spectra [7, 14, 15]. These techniques provide adequate structural information for the identification and confirmation of pesticides in environmental samples [6, 14].

In the present study, the mass spectrometric analysis of a series of *N*-substituted amine and anilide, carbamate and thiocarbamate, phenylurea, phosphate, phosphonate, sulfonylurea and thiourea, and triazine and other *N*-heterocyclic pesticides is reported. HPLC in conjunction with thermospray ionization was used for monitoring environmental samples. One aim of the present study is to extend the multiresidue method we reported previously [6], where mainly full-scan experiments were performed. Therefore, additional pesticides were included and time-scheduled selected ion monitoring (SIM) experiments were performed.

Furthermore, a variety of methods are proposed that enhance the structural information from TSP spectra. Thus, the TSP spectra of sulfonylureas, anilides, and *N*-substituted amines show abundant fragmentation, which is formed either by thermal degradation of the neutral molecule followed by ionization or by decomposition of the quasimolecular ion. Comparison of the TSP spectra with ESI, fast-atom bombardment (FAB), and ^{252}Cf plasma desorption (^{252}Cf-PD) spectra [and collision-activated dissociation (CAD) spectra of the quasimolecular ions] has been used for elucidating the degradation mechanism. The fragmentation level is lower with phenylureas, but a structural specific fragment also is observed that may be used to confirm a tentative identification based on the quasimolecular ion. APCI, ESI, and FAB spectra are again used to confirm the proposed pathways. Finally, for triazines and several *N*-heterocyclic compounds, which hardly show any fragmentation under TSP ionization, postcolumn addition of different alkylated amines to the carrier stream is applied to induce on-line derivatization reactions in the condensed phase of the vaporizer probe. Furthermore, by applying postcolumn on-line derivatization (POD), additional clustering and fragmentation reactions are observed for carbamates, phenylureas, and *N*-heterocyclic compounds in combination with solvent-mediated chemical ionization (CI).

Experimental

Materials and Reagents

The pesticide standards used in this work were purchased from Riedel-de Haen (Seelze-Hannover, Germany) and Promochem (Wesel, Germany) and ranged in purity from 97 to 99.5%. Standards of the sulfonylurea herbicides were provided by E. I. du Pont de Nemours (Bad Homburg, Germany) and Ciba-Geigy (Frankfurt, Germany) except chlorosulfuron and metsulfuron-methyl (Riedel-de Haen). Methanol (HPLC grade, Riedel-de Haen) and purified water (Milli-Q water, Millipore, Bedford, MA) were used as solvents. Ammonium acetate was purchased from Aldrich (Steinheim, Germany), and polyethylene glycol 300 and 400, the alkylated amines, and caffeine were purchased from Fluka (Buchs, Switzerland).

Sample Preparation

The pesticides were extracted from water (1 L, 10 mL min^{-1}) by using solid-phase extraction cartridges filled with 3-g C-18 material (Amchro, Sulzbach-Taunus, Germany). Four 2-mL methanol washes carried the pesticides trapped on the cartridge to a sample vial. Thereafter, the volume was reduced to $\approx$ 500 μL by using a gentle stream of nitrogen. Finally, the internal standard (caffeine) was added and 50 μL of the extract was injected into the LC-MS system. Alternatively, direct on-line enrichment with subsequent desorption to the analytical column was performed with a self-constructed on-line extraction apparatus. In these experiments, 50–200 mL of the water sample were passed through a 10- × 2-mm cartridge (Spark, The Netherlands) filled with ~ 40-mg C-18 material (Amchro). Desorption to the analytical column is achieved via

elution with the initial gradient composition after column switching with a pneumatic six-port valve (Valco, Houston, TX).

Liquid Chromatography

Details of the experimental setup are described elsewhere [7]. Briefly, a postcolumn technique was employed to enhance sensitivity and selectivity. The liquid chromatography (LC) system consisted of a Varian (Palo Alto, CA) Model 5000 gradient liquid chromatograph and a Shimadzu (Kyoto, Japan) Model LC-9A pump for the postcolumn addition of reagent solution. Narrow bore 3-mm columns with a column flow rate of 0.6 mL min^{-1} were used. An additional flow rate of 0.4 mL min^{-1} of a reagent solution was added postcolumn. The reagent solution consisted of 175-mM aqueous ammonium acetate or, in some instances, additional reagent additives. LiChrocart cartridge columns (125 × 3 mm i.d.) packed with 5-μm LiChrospher 60 RP-select B from Merck (Darmstadt, Germany) were used. Separation was accomplished by using the following eluent composition: methanol : water = 20 : 80 (v/v) was programed to 95 : 5 in 45 min. The final composition was held for 15 min. To keep the sulfonylureas, asulam, and bentazone in an undissociated form, they were separated with an acidified mobile phase. In this case, 100-mM acetic acid was used instead of pure water. A 7125 injection valve (Rheodyne, Cotati, CA) equipped with a 20- or 50-μL loop was used to introduce the samples. To avoid peak broadening of early eluting compounds it is recommended that the sample solutions be injected with a high water content ($\geq$ 80%).

Mass Spectrometry

Many details of the TSP LC-MS configuration and operation have been reported earlier [6, 7]. Briefly, a Finnigan-MAT 4500 mass spectrometer (Finnigan-MAT, San Jose, CA) was coupled with the LC system via a Vestec thermospray source (Houston, TX). The TSP temperatures were vaporizer control $T_1 \approx$ 135–150 °C, vaporizer $T_v \approx$ 190–220 °C, tip heater T_3 = 270 °C, source jet (vapor) $T_g \approx$ 230–240 °C, and source T_s = 250 °C. Discharge-assisted buffer ionization with ammonium acetate was used throughout all quantification experiments. The terms "thermospray ionization" and "solvent-mediated CI" are used as described by Niessen and Van der Greef [21], that is, thermospray ionization refers to buffer ionization with a volatile salt and solvent-mediated CI refers to discharge ionization without buffer. In the present article both terms are also used to differentiate between the postcolumn ionization conditions obtained if either pure alkylated amines (solvent-mediated CI) or their corresponding acetates (discharge-assisted buffer ionization) are added to the carrier stream. The discharge-assisted buffer ionization spectra are consistent with those obtained under normal TSP ionization, although in some cases a somewhat higher fragmentation is observed (see examples in the following text), whereas discharge-assisted buffer ionization and solvent-mediated CI often exhibit very different spectra [6].

Direct flow injection experiments were performed by using a final carrier stream of methanol : water = 50 : 50 (v/v) and postcolumn addition of 70-mM ammonium acetate (the column and postcolumn flow rates are the same as those used for the HPLC separations). In several experiments, ammonium acetate is replaced by different organic modifiers that are added postcolumn and, again, with a concentration of 70 mM.

The lower limit of the mass spectrometer scan range depends on the solvent cluster ion spectrum and thus the organic modifier used. Usually, the mass spectrometry was either scanned at a rate of 1 s per scan over the range m/z 120–450 (positive ions) and m/z 185–500 (negative ions) or time-scheduled selected ion monitoring (SIM) was performed.

Low energy tandem mass spectrometry experiments were carried out on a Finnigan-MAT TSQ 70 triple-stage quadrupole mass spectrometer (Q1, Q2, Q3) equipped with a Finnigan-MAT thermospray source. Collision-activated dissociation (CAD) was achieved within the rf-only quadrupole, where a collision offset (COFF) of 20 V was applied to Q2. Argon was used as the collision gas with a collision cell pressure of 1.3 × 10^{-3} torr. Direct flow injection was used to introduce the samples into the mass spectrometer. The carrier stream consisted of methanol : water = 50 : 50 (v/v) containing 50-mM ammonium acetate. The aerosol temperature, T_g', was kept at 240 °C, while the vaporizer control temperature T_1' was varied between 70 and 95 °C.

Fast-atom bombardment (FAB) spectra were recorded on a Finnigan-MAT 8430 double-focusing mass spectrometer. 3-Nitrobenzyl alcohol (NBA) was used as the matrix in most instances. If the samples were not soluble in NBA or chemical reactions with NBA occurred, a glycerol matrix was used. Sample concentrations of $\sim$ 500 ng per microliter of NBA were used. The samples were admitted by means of the standard direct-inlet probe carrying a stainless steel target. The scan speed was 3 s $decade^{-1}$. Ions were produced by an 8-keV primary beam of xenon atoms, extracted and accelerated with an 8-kV potential. NBA exhibits intense matrix ions at m/z 136, 154, 176, 289, 307, and 329.

^{252}Cf plasma desorption (^{252}Cf-PD) mass spectra were recorded on a Bion-Ion Nordic AB (Uppsala, Sweden) plasma desorption time-of-flight (TOF) mass spectrometry system using a Mylar® (Alexander Vacuum Research, Boston, MA) film as target. Approximately 5 μL of the sample solutions (concentration $\sim$ 300 ng μL^{-1} in methanol) were deposited on the Mylar foil.

Electrospray and APCI experiments of phenylureas and sulfonylureas were performed on a Finnigan-MAT TSQ 700 mass spectrometer equipped with either an ESI or APCI source. With APCI, a vaporizer temperature of 400 °C was used. The samples were introduced into the ESI and APCI source with a carrier flow rate of 300 μL min^{-1} after separation on a minibore 125-× 2-mm (5-μm) LiChrospher 100 RP-18 column (Merck). Solvents and gradient conditions were identical to those used in the TSP LC-MS investigation. Ammonium acetate was added to the carrier stream in some instances to enhance ionization (see text). The ESI spectra of the anilides were recorded on a triple-stage Perkin Elmer Sciex (Thornhill, Ontario, Canada) API III quadrupole mass spectrometer equipped with an electrospray source. Direct flow injection was used to introduce the samples into the carrier stream [methanol : water = 50 : 50 (v/v); flow rate 50 μL min^{-1}] in these samples.

Results and Discussion

A series of nitrogen- and phosphorus-containing pesticides was investigated by positive-ion thermospray LC-MS, as summarized in Table 1. The sulfonylureas and most of the phenylureas, the phosphonates, many carbamates, and certain amines cannot be analyzed by GC mass spectrometry because of their thermal instability and polarity. Therefore, these compounds were the preferred choice for LC-MS investigations. Other selected compounds lack a strong chromophore and thus cannot be detected at trace level with conventional LC UV detection. This is particularly the case for several amines and carbamates, for example, aldicarb, allidochlor, EPTC, mecarbam, methomyl, oxamyl, pebulate, propamocarb, thiofanox, thiodicarb, triallate, and vernolate, and the organophosphorous compounds investigated. Many typical "GC pesticides" are also amenable to TSP and HPLC. These compounds were also included to demonstrate the universality of the method.

Evaluation of the Method

We previously demonstrated the TSP LC-MS analysis of 95 pesticides using one common method with a single set of experimental parameters and full-scan mass spectrometry [6]. The former study showed that the reproducibility, linearity, and instrumental detection limits obtained were adequate for environmental monitoring of a broad spectrum of pesticides without necessitating the use of isotopically labeled internal standards.

Assuming a two-thousandfold concentration step via solid-phase extraction and an injection volume of 50 μL into the LC system, a ~ 5–10-ng amount has to be detected via TSP after LC separation to verify the CEC drinking water level (100 ng L^{-1}). However, for several pesticides this criterion could not be achieved with full-scan analysis. In the present study the experiments were extended to time-scheduled SIM measurements to lower the detection limit of the method to the low parts-per-trillion range. In addition, new compounds are included in the list, for example, sulfonylureas and several thiocarbamates.

A typical TSP full-scan chromatogram of a standard solution of 27 carbamates and thiocarbamates is shown in Figure 1 (injected amount, ~ 180 ng each). During all chromatographic experiments, caffeine was added as an internal standard.

A list of the retention times of 50 important pesticides is presented in Table 2 together with their ammonium acetate TSP quantitation ions, second most abundant fragment or cluster ions, and detection limits (LOD) obtained by time-scheduled SIM. Verification of the CEC limit concentration is quite possible for all investigated compounds under these conditions. Most of the pesticides can be detected down to the lower picogram range per compound injected into the column. This is demonstrated in Figure 2, where the time-scheduled SIM trace for the injection of 100 pg of four phenylureas is shown (Table 2 lists the corresponding quantitation ions). Similar detection limits also are observed for triazines and many carbamates.

In general, although sensitivities varied widely from compound to compound (Table 2), positive-ion TSP analysis was more sensitive than negative-ion analysis, the results of which are not shown in this report. However, in some instances the combination of both ionization modes provides valuable additional structural information for the characterization of pesticides as previously reported for carbamates [7].

Analysis of a River Water Extract

In this section, an example for the parts-per-trillion level determination and confirmation of several phenylureas from a spiked river water sample is shown. The unambiguous identification of phenylureas is more difficult than that of many other pesticides because they lack intense fragment ions in the "usual" TSP scan range of m/z 120–450. However, in the case of *N,N*-dimethylureas, such confirmation is possible by using the abundant fragment ion at m/z 46 to confirm the identification based on the quasimolecular ion (the origin of this ion is described in more detail below). This is demonstrated in Figure 3, where the results of two TSP LC-MS separations of an extract of a water sample (river water) are shown. The original water sample was spiked with nine phenylureas at a concentration of 100 ng L^{-1} (CEC limit). Preconcentration was achieved via solid-phase extraction. Fifty microliters of the methanol extract were injected. The separation and mass spectrometry detection were per-

Table 1. Pesticides and some of their transformation products investigated in this study

Anilides and *N*-substituted amines	Carbamates and thiocarbamates
Alachlor	Aldicarb
Allidochlor	Aldicarb sulfone
Bentazone	Aldicarb sulfoxide
Butachlor	Asulam
Carboxin	Barban
Dimethachlor	Benomyl
Oxicarboxin	Carbaryl
Metalaxyl	Carbetamide
Metazachlor	Carbofuran
Methfuroxam	Chlorpropham
Metolachlor	Desmedipham
Monalide	EPTC
Pendimetalin	Mecarbam
Pentanochlor	Methiocarb
Prochloraz	Methomyl
Propachlor	Oxamyl
Propanil	Pebulate
Tebutam	Phenmedipham
Trifluralin	Pirimicarb
	Promecarb
Phenylureas and thioureas	Propham
Chlorbromuron	Propoxur
Chlorotoluron	Prosulfocarb
Chloroxuron	Pyridate
Difenoxuron	SWEP
Diuron	Thiodicarb
Fenuron	Thiofanox
Fluometuron	Triallate
Isocarbamide	Vernolate
Isoproturon	
Linuron	Sulfonylureas
Metabenzthiazuron	Bensulfuron-methyl
Metobromuron	Chlorimuron-methyl
Metoxuron	Chlorsulfuron
Monolinuron	Metsulfuron-methyl
Monuron	Primisulfuron-methyl
	Sulfometuron
Triazines and *N*-heterocyclic compounds	Thifensulfuron-methyl
Ametryn	Tribenuron-methyl
Anilazine	
Atratone	Organophosphorous compounds
Cyanazine	Butonate
Desmetryn	Dichlorovos
Metribuzine	Trichlorfon
Prometryn	
Propazine	
Secbumetone	
Sebutylazine	
Simazine	
Terbutylazine	
Terbutryn	

formed with time-scheduled SIM of the $[MH]^+$ ions and the ion at m/z 46. Identification and confirmation of the *N,N*-dimethyl-phenylureas are quite possible even at this low concentration. [The time window for difenoxuron (peak 8) at m/z 287 is not applied in the time-scheduled SIM analysis (Figure 3a) because the retention time is very similar to peak 7. However, Figure 3b indicates the presence of difenoxuron.] Slight differences in retention times between Figure 3a and b are due to the separate chromatographic analyses. Therefore, in critical cases both ions should be included in one time window during time-scheduled SIM.

Figure 3 and Table 2 clearly demonstrate that iden-

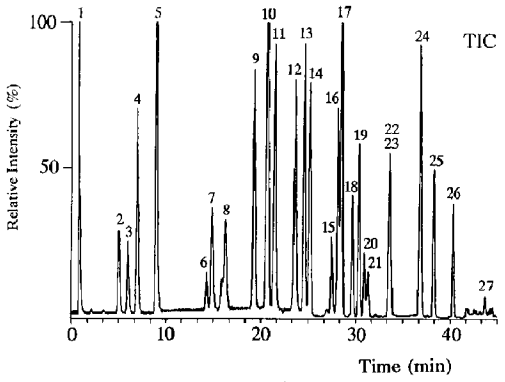

Figure 1. Discharge-assisted TSP chromatogram of 27 carbamates and thiocarbamates and some of their degradation products under full-scan conditions (injected amount: 180 ng each). Experimental conditions: $T_g \approx 235$ °C, $T_v = 220 \rightarrow 209$ °C. For details, see Experimental section. Peak assignments: 1, asulam; 2, aldicarb sulfone; 3, methomyl; 4, oxamyl; 5, caffeine (internal standard); 6, 3-methoxy-carbonyl-aminophenylalcohol; 7, benomyl; 8, aldicarb; 9, carbetamide; 10, propoxur; 11, carbofuran; 12, carbaryl; 13, pirimicarb; 14, propham; 15, thiodicarb; 16, desmedipham; 17, phenmedipham; 18, chlorpropham; 19, promecarb; 20, methiocarb; 21, barban; 22, SWEP; 23, EPTC; 24, pebulate/vernolate; 25, prosulfocarb; 26, triallate; 27, pyridate.

tification, quantification, and confirmation are quite possible in this low concentration range for almost all of the investigated pesticides.

Enhancing Structural Information from Thermospray Spectra and Confirmation of Pesticide Residues. Application of Other Ionization Techniques

Triazines and other N-heterocyclic compounds. Thermospray and solvent-mediated CI spectra of triazines, pyrimidines, triazoles, and many other compounds that contain an *N*-heterocyclic moiety are usually very simple and consist in general only of $[MH]^+$ ions because of their high proton affinity in comparison to ammonia, methanol, or water. The lack of structurally significant fragments limits the specificity of analysis. Voyskner [11] demonstrated the usefulness of tandem mass spectrometry techniques in the analysis of chlorotriazines to overcome this problem. In this study we report an alternative approach to enhance structural information from chlorotriazine spectra by using postcolumn on-line derivatization (POD) reactions in the condensed phase of the vaporizer probe. These derivatizations are performed in combination with solvent-mediated chemical ionization via discharge ionization or normal TSP ionization. POD leads on the one hand to a chlorine substitution by the amine, and on the other hand to adduct ion formation. Both processes are useful to enhance structural information from TSP spectra and thus the selectivity of the method.

POSTCOLUMN DERIVATIZATION OF CHLOROTRIAZINES WITH ALIPHATIC AMINES. The TSP spectra of monochlorotriazines exhibit unusual $[M - 5]^+$ and $[M + 9]^+$ ions with no chlorine isotope pattern when methylamine and dimethylamine, respectively, are added postcolumn to the carrier stream instead of the usual ammonium acetate. Figures 4 and 5 demonstrate the influence of different additives on the ion abundance of atrazine and anilazine (see also Experimental section). Other chlorotriazines, such as cyanazine, propazine, sebutylazine, simazine, and terbutylazine, behave similarly. Table 3 summarizes these results for the chlorotriazines investigated as well as further results obtained with structurally different triazines.

Obviously, a nucleophilic substitution of the chlorine atom takes place as is typical for π-deficient heteroaromatics. These substitutions most probably occur as condensed-phase reactions in the vaporizer probe prior to ionization and most likely are assisted by heat and solvent, that is, the TSP interface is used as a flow reactor for the derivatization reactions. Structurally specific ions, viz. $[M - Cl + HNCH_3 + H]^+$ ($= [M - 5]^+$) and $[M - Cl + N(CH_3)_2 + H]^+$ ($= [M + 9]^+$), are observed. The extent of substitution depends on the structure of the triazine and the nucleophilicity of the amine. Therefore, by adding dimethylamine, higher reaction yields are obtained (Table 3) and a complete substitution usually occurs. POD reactions are observed in both the TSP and the solvent-mediated CI mode with an identical extent of substitution. In the discharge mode, additional $[MH - 34]^+$ and $[M_sH - 34]^+$ ions, respectively, are observed that result from a loss of a chlorine atom, where M_s is the protonated POD product ion. These $[M - Cl + 2H]^+$ and $[M_s - Cl + 2H]^+$ ions are formed by substitution of a chlorine atom by a hydrogen atom. This fragmentation is discussed in more detail below.

If an equimolar amount of acetic acid is added to the postcolumn amine solution (discharge-assisted buffer ionization) the signal for $[M - Cl + HNCH_3 + H]^+$ and $[M - Cl + N(CH_3)_2 + H]^+$ almost disappears (Figure 4a and b). This behavior is consistent with the proposed nucleophilic substitution because methylammonium acetate and dimethylammonium acetate do not exhibit nucleophilicity.

The spectrum of anilazine shows POD product ions that are due to the substitution of both chlorines bound to the heterocyclic aromatic ring. As expected, the phenyl-bound chlorine is not substituted by the nucleophilic reagents. (Loss of this chlorine atom may be observed under certain experimental conditions. This loss is due to a radical reductive dechlorination prior to ionization. However, this reaction occurs with all reagent additives and is only induced by the CI plasma. For details, see below.) The signal at m/z 256 in the spectrum of anilazine (Figure 5a) with ammonium acetate as the additive apparently corresponds to a POD product obtained by chlorine–ammonia substitution.

Table 2. Elution order, main positive ions, and SIM detection limits (LOD) in the TSP LC-MS analysis of important pesticides and some of their transformation products

No.	Compound Common name	M_n[a]	Retention time (min)	Quantitation ion	Second ion[b]	LOD (pg)[c]
1	Aldicarb sulfoxide	206	4.10	224	207(65)	500
2	Aldicarb sulfone	222	4.27	240	165(70)	600
3	Oxamyl	219	5.48	237	163(20)	300
4	Methomyl	162	6.68	163	180(10)	200
5	Caffeine[d]	194	8.50	195	—	70
6	Fenuron	164	10.77	165	182(40)	50
7	Isocarbamide	185	15.00	186	146(5)	100
8	Benomyl	290	15.05	192	134(90)	300
9	Allidochlor	173	15.97	174	191(15)	50
10	Aldicarb	190	16.27	208	191(30)	200
11	Metoxuron	228	17.47	229	201(8)	300
12	Monuron	198	20.05	199	171(5)	100
13	Propoxur	209	20.77	227	210(20)	100
14	Carbofuran	221	21.57	222	239(35)	70
15	Carbaryl	201	23.72	219	202(18)	80
16	Monolinuron	214	23.85	215	232(10)	60
17	Pirimicarb	251	24.58	252	—	40
18	Chlorotoluron	212	24.92	213	185(5)	40
19	Metobromuron	258	25.11	259	276(10)	200
20	Propham	179	25.42	197	180(90)	60
21	Metabenzthiazuron	221	25.98	222	165(17)	200
22	Metazachlor	277	26.03	278	244(8)	100
23	Isoproturon	206	26.28	207	179(12)	100
24	Propachlor	211	26.30	212	229(10)	200
25	Metalaxyl	279	26.52	280	—	300
26	Atrazine	215	26.73	216	182(10)	90
27	Dimethachlor	255	27.00	256	222(38)	300
28	Diuron	232	27.08	233	250(10)	100
29	Methfuroxam	229	27.52	230	—	200
30	Difenoxuron	286	27.65	287	216(68)	100
31	Desmedipham	300	28.38	199	137(60)	100
32	Phenmedipham	300	28.67	185	168(45)	90
33	Carbetamide	236	28.73	237	177(28)	200
34	Linuron	248	29.92	249	266(18)	70
35	Chlorpropham	213	30.00	231	214(30)	200
36	Terbutylazine	229	30.30	230	196(10)	100
37	Propanil	217	30.80	218	235(65)	300
38	Methiocarb	225	31.38	243	226(65)	100
39	Barban	257	31.78	275	258(10)	300
40	Mecarbam	329	32.01	330	347(20)	200
41	Chloroxuron	290	32.18	291	220(20)	90
42	Alachlor	269	32.93	270	226(88)	400
43	Metolachlor	283	33.40	284	250(33)	200
44	Monalide	239	34.17	240	—	200
45	Pentanochlor	239	35.63	240	257(5)	200
46	Pendimetalin	281	35.88	282	220(50)	300
47	Prochloraz	375	36.25	376	180(90)	200
48	Trifluralin	335	36.55	276	336(80)	300
49	Prosulfocarb	251	38.80	239	—	100
50	Triallate	303	40.93	304	162(20)	100
51	Butachlor	311	41.10	226	238(95)	300

[a] M_n = nominal mass.
[b] This column lists the most abundant structurally significant fragment ion or molecule cluster ion, although in some instances isotopic peaks of the quantitation ion are more abundant. The abundance in parentheses is listed relative to the quantitation ion (base peak).
[c] Signal-to-noise ratio = 3. The values are cited to one significant figure.
[d] Internal standard.

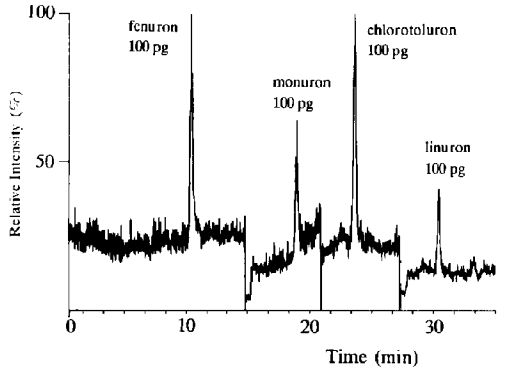

Figure 2. Discharge-assisted TSP LC-MS analysis of phenylureas: time-scheduled SIM trace for the injection of 100 pg of each compound.

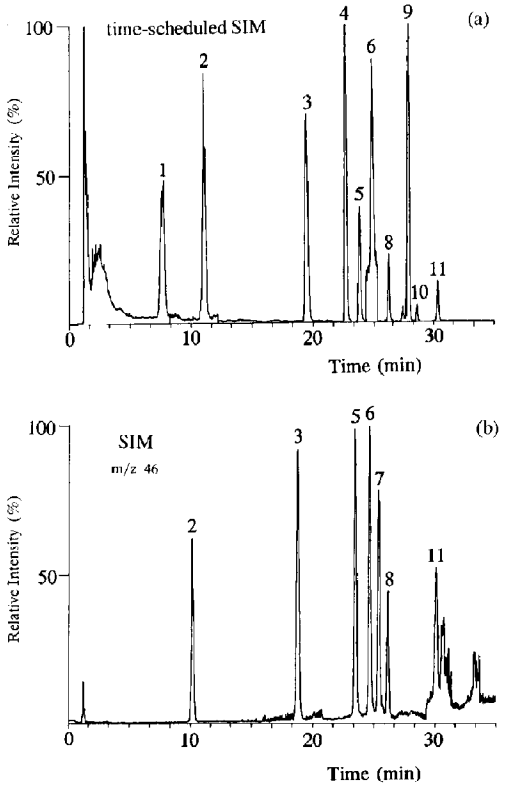

Figure 3. Analysis of a river water extract (River Leine, Hannover) by TSP LC-MS. The original water sample was spiked with phenylureas at the 100 ng L^{-1} level. Peak assignments: 1, caffeine; 2, fenuron; 3, monuron; 4, linuron; 5, chlorotoluron; 6, isoproturon; 7, diuron; 8, difenoxuron; 9, linuron; 10, chlorbromuron; 11, chloroxuron. (a) Time-scheduled SIM TSP chromatogram of the $[MH]^+$ ions; (b) confirmation of *N,N*-dimethyl-phenylureas. The SIM trace of protonated dimethylamine is formed from dissociation of the phenylurea to its $[MH - PheNCO]^+$ ion (m/z 46).

The mechanism for the chlorine–hydrogen substitution in the POD spectrum of atrazine obtained with trimethylammonium acetate that leads to the ion at m/z 182 is not yet clear (Figure 4c). Furthermore, the sensitivity obtained with this reagent is not satisfactory for analytical purposes (Table 4).

As expected, alkylthiotriazines and alkoxytriazines do not undergo nucleophilic substitution, as can be seen from Table 3.

Although the reactions described strongly depend on the interface temperatures and therefore careful adjustment of the temperatures is necessary for reproducible results, the reactions can be induced over the entire operating range of the TSP interface, viz. $T_v \approx$ 160–230 °C and $T_g \approx$ 190–290 °C. However, isobaric and isomeric compounds, for example, propazine and terbutylazine could not be distinguished from their POD spectra. That is, tandem mass spectrometry should be applied in these cases [11].

CLUSTER ION FORMATION. In some instances, alkylammonium cluster ions of triazines are observed, especially if trimethylamine is added (Figure 4 and Table 3). This is due to the higher proton affinity of the alkylamines, PA(B), as compared to ammonia. Hence protonation of the triazines is less exothermic and attachment of the ionizing cluster ions becomes more favored. We have investigated the effect of the proton affinity on the ion abundance of several compounds in the range PA(B) = 853–942 kJ mol^{-1} by applying post-column addition of various alkylated amines. The reagents used are summarized in Table 4. All proton affinities are from Lias and co-workers [22, 23].

The TSP reagent ion spectra of the postcolumn mixtures under thermospray and discharge ionization are very simple and usually consist of only $[amine \cdot H]^+$, $[amine \cdot CH_3OH \cdot H]^+$, and $[(amine)_2 \cdot H]^+$ ions if pure amine is added, whereas the spectra of the corresponding acetates contain additional ions, which are due to clusters of these ions with acetic acid, *N*-alkylacetamide, water, and methanol and mixtures of these ions, respectively.

The spectra of several *N*-heterocyclic compounds undergo a "transition" from the $[MH]^+$ ion to the $[M \cdot H \cdot amine]^+$ ion, if the PA is changed (the PA of these compounds are within the investigated range of PA(B) = 853–942 kJ mol^{-1}). As an example, the effect of the proton affinity on the spectra of the triazinone pesticide metribuzine is summarized in Figure 6, where the ratio of the ion current of the $[MH]^+$ ion relative to the adduct ion $[M \cdot H \cdot amine]^+$, $r(M)$, is plotted against PA ($r(M)$ is defined as described in [7]). A strong shift to the $[MH]^+$ ion is observed with decreasing PA. Ionizing with ammonia usually leads to the regular TSP spectra of *N*-heterocyclic compounds, that is, only the $[MH]^+$ ion is formed. The correlation is valid for both the pure alkylated amine and the alkylammonium acetate, that is, identical spectra are observed.

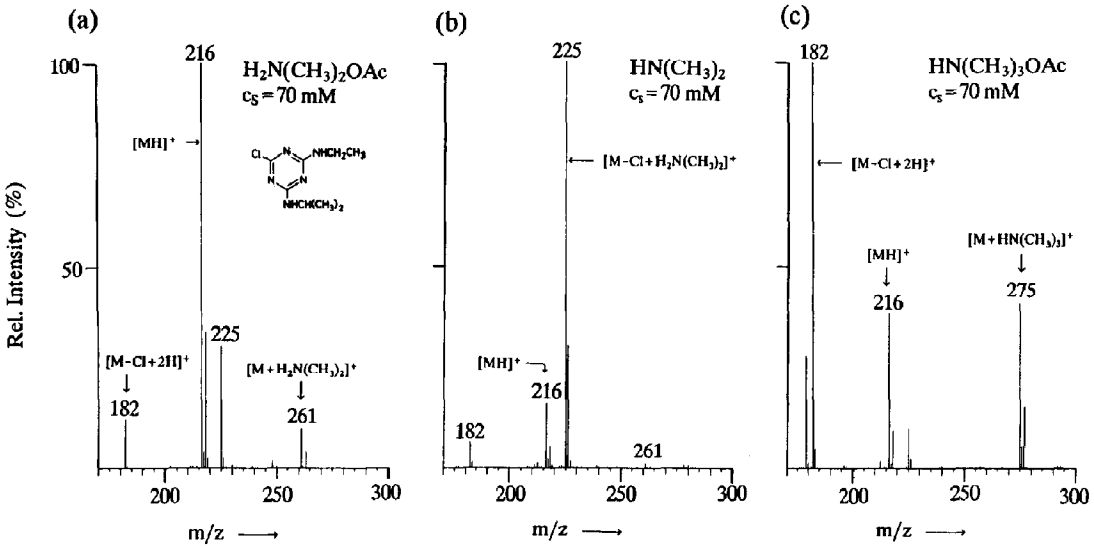

Figure 4. Thermospray postcolumn on-line derivatization (POD). Variation of ion abundances in TSP mass spectra with condensed-phase nucleophilicities and gas-phase proton affinities. POD spectra of atrazine: postcolumn addition of (a) dimethylammonium acetate (discharge-assisted TSP), (b) dimethylamine (solvent-mediated CI), and (c) trimethylammonium acetate (discharge-assisted TSP).

These cluster ions may be of value in TSP SIM analysis of environmental samples, for example. In some instances, we observed a very noisy baseline for some ions during SIM experiments with ammonium acetate. Although the absolute ion itensities are not affected, the signal-to-noise ratios are unsatisfactory in such instances. This behavior is due to either an interfering solvent cluster ion of high mass or, more probably, to a contamination of the source after repetitive injection of sample extracts. In such instances it is very useful to switch to an alternative ion of equal or comparable intensity for quantitation. This is especially important for pesticides with proton affinities in the range of ammonia, that is, for most carbamates, phenylureas, anilides, and organophosphorous compounds. These compounds form almost exclusively $[M \cdot H \cdot amine]^+$ ions by ionization with protonated alkylated amines. Therefore, it is important to compare

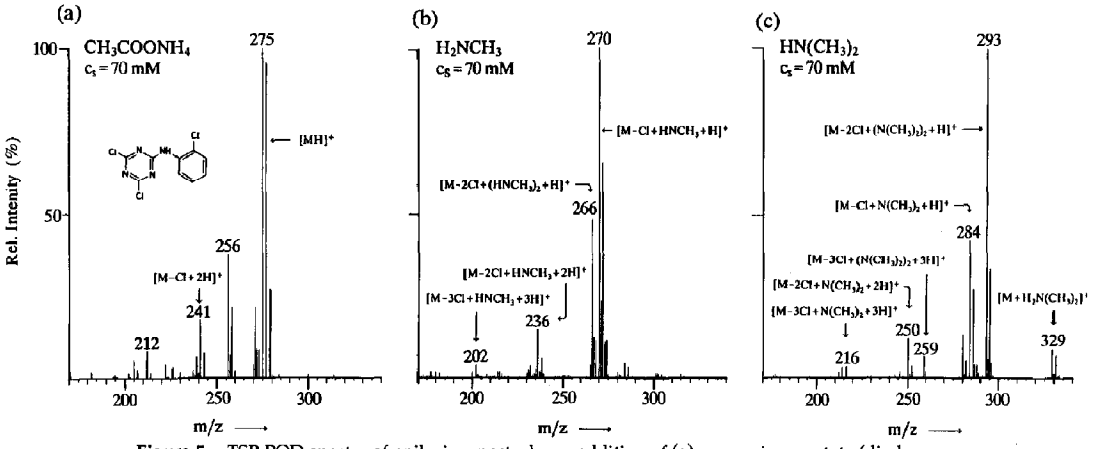

Figure 5. TSP POD spectra of anilazine: postcolumn addition of (a) ammonium acetate (discharge-assisted buffer ionization), (b) methylamine (solvent-mediated CI), and (c) dimethylamine (solvent-mediated CI).

Table 3. Summary of POD mass spectral data obtained from the solvent-mediated CI (discharge) analysis of triazines after postcolumn addition of methylamine and dimethylamine[a]

Compound	M_n	$[MH]^+$[b]	CH_3NH_2			$(CH_3)_2NH$		
			$[M_sH]^+$[c]	γ (%)[d]	Adduct[e]	$[M_sH]^+$	γ(%)	Adduct
Chlorotriazines								
Anilazine[f]	274	275	266/70	100	—	284/93	100	329(15)
Atrazine	215	216	211	3	—	225	76	261(3)
Cyanazine	240	241	236	5	272(35)	250	45	286(25)
Propazine	229	230	225	5	—	239	82	273(3)
Sebutylazine	229	230	225	2	—	239	27	275(4)
Simazine	201	202	197	12	—	211	97	—
Terbutylazine	229	230	225	5	—	239	85	275(1)
Alkylthiotriazines								
Ametryn	227	228	—	0	—	—	0	—
Desmetryn	213	214	—	0	—	—	0	—
Prometryn	241	242	—	0	—	—	0	—
Terbutryn	241	242	—	0	—	—	0	—
Alkoxytriazines								
Atratone	211	212	—	0	—	—	0	—
Secbumetone	225	226	—	0	—	—	0	—

[a]For experimental conditions, refer to Table 4.
[b]Mass-to-charge ratio of the protonated precursor compound.
[c]Mass-to-charge ratio of the protonated substitution product: $[M_sH]^+ = [M - Cl + NHCH_3 + H]^+$ (methylamine); $[M_sH]^+ = [M - Cl + N(CH_3)_2 + H]^+$ (dimethylamine). Note that in the discharge-assisted TSP spectra that use $CH_3CO_2NH_4$ the $[MH]^+$ ion is always the base peak and no other ions except the $[M - Cl + 2H]^+$ are present.
[d]Substitution is defined in terms of relative abundances: $\gamma = \Sigma([M_sH]^+ + [M_s - Cl + 2H]^+)/([MH]^+ + [M_sH]^+ + [M_s - Cl + 2H]^+ + [M \cdot H \cdot amine]^+) \times 100$ (it is assumed that the ionization efficiency is approximately the same for M and M_s). Values represent the means of at least three determinations.
[e]$[M \cdot H \cdot amine]^+$ (% abundance relative to the base peak $[MH]^+$ or $[M_sH]^+$). Anilazine exhibits $[M_s \cdot H \cdot amine]^+$ ions.
[f]Substitution of two chlorine atoms.

the sensitivities obtained by adding different postcolumn mixtures with that obtained with ammonium acetate. Table 4 summarizes these results for the different ionization modes applied to the carbamate pirimicarb, which contains an *N*-heterocyclic moiety. Observe that only amines of lower molecular weight give satisfying results, which are comparable to ammonium acetate. In addition, solvent-mediated CI yields higher sensitivities than discharge-assisted buffer ionization. The relative sensitivities shown in Table 4 are typical for all investigated compounds.

Similar considerations hold for POD reactions, that is, only methylamine and dimethylamine should be used in analytical applications. Ionizing with a mixture of methylamine or dimethylamine and ammonium acetate is not advantageous: although the sensitivity is

Table 4. Comparison of TSP, discharge-assisted buffer ionization, and solvent-mediated CI sensitivities for pirimicarb obtained by postcolumn addition of several alkylated amines and their acetates[a]

Amine[b]	M_n	PA[c]	R_3N		$R_3N \cdot H \cdot OAc$	
			SMCI[d]	TSP	DATSP[e]	TSP
NH_3	17	853	—	—	100	30
CH_3NH_2	31	896	95	12	61	6
$(CH_3)_2NH$	45	923	87	9	50	9
$(CH_3)_3N$	59	942	38	4	35	< 1
$C_2H_5NH_2$	45	908	79	3	66	10
$i - C_3H_7NH_2$	59	915	60	6	43	7
$t - C_4H_9NH_2$	73	924	30	5	20	5
$n - C_5H_{11}NH_2$	87	916	21	5	20	5
$n - C_6H_{13}NH_2$	101	920	14	5	12	3

[a]All values are given relative to the sensitivity obtained by discharge-assisted buffer ionization with ammonium acetate (= 100%) (average of at least three injections).
[b]All experiments are performed under identical experimental conditions, that is, $T_v = 202$ °C (≅ 95% vaporization), $T_g = 235$ °C; direct flow injection; amount injected, 500 ng; carrier stream methanol : water = 50:50 (v/v) with $c_s = 70$ mM after postcolumn addition of reagent solution; see also Experimental section.
[c]Proton affinity in kilojoules per mole.
[d]SMCI = solvent-mediated CI.
[e]DATSP = discharge-assisted buffer ionization.

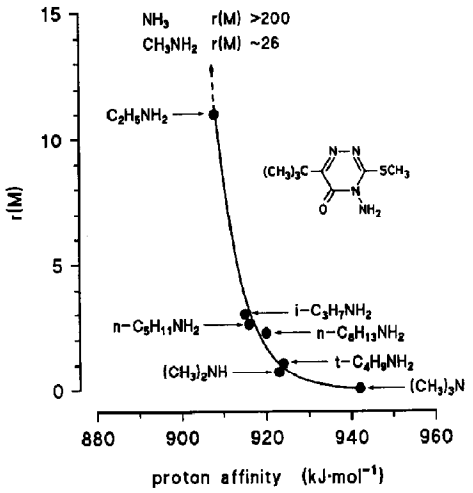

Figure 6. The dependence of adduct formation in TSP spectra on the proton affinity of the reagent ions. The relationship is shown for metribuzine; $r(M) = I(MH^+)/I(M \cdot adduct^+)$. For details, refer to the text.

enhanced and comparable to that achieved with pure ammonium acetate, the POD substitution of chlorotriazines is almost completely suppressed.

Finally, if unknown compounds in real samples are identified by normal TSP-MS in a first step, the additional cluster formation described above is useful to confirm this identification in a second step.

Phenylureas

FRAGMENTATION. *N,N*-dimethyl-phenylureas show characteristic $[M - 11]^+$, $[M - 28]^+$, and (less intense) $[M - 45]^+$ ions under discharge-assisted ammonium acetate ionization. These ions are due to the isocyanate formed from the thermally labile phenylureas and they probably correspond to the $[M - HN(CH_3)_2 + NH_3 \cdot NH_4]^+$, $[M - HN(CH_3)_2 + NH_4]^+$, and $[M - HN(CH_3)_2 + H]^+$ ions. Thermal decomposition of trisubstituted urea pesticides under gas chromatographic conditions has been reported [24].

The unusual adduct ion $[\text{isocyanate} + NH_3NH_4]^+$ in the TSP spectra was also reported by Cairns and Siegmund for neburon [25]. Generally, isocyanates exhibit less intense proton adducts due to their low proton affinity. $NH_3NH_4^+$ adduct ions of isocyanates were also observed in the TSP spectra of carbamates, for example, in the case of desmedipham, where the ion at m/z 154 reported previously [6] probably corresponds to the $NH_3NH_4^+$ adduct ion of phenylisocyanate. Alternatively, the structure of the $[\text{isocyanate} + NH_3NH_4]^+$ ion can be assigned to $[RNHCONH_2 \cdot H \cdot NH_3]^+$, which may be formed from the reaction between isocyanate and ammonia or ammonium-containing species in the reagent flow followed by ionization via ammonium attachment.

However, the relative abundance of isocyanate-related ions in the spectra of *N,N*-dimethyl-phenylureas is rather low as compared to the quasimolecular ions and usually does not exceed 10%. Furthermore, in most cases the protonated amine formed is much more intense. Particularly the TSP spectra of *N,N*-dimethyl-phenylureas show ions due to protonated dimethylamine (m/z 46) with relative abundances up to 80%. Scheme I shows the different ionic species observed, where only the proton adducts of the decomposition products are represented. These ions are summarized in Table 5 for several phenylureas. (In addition, this table contains the results obtained by APCI, ESI, and FAB ionization as discussed below.) Although these ions are less specific, they can be used as confirmatory ions in combination with SIM, because no other intense fragment ions are available under normal operating conditions and no interfering signal is present in the reagent ion spectra of methanol–water–ammonium acetate mixtures at m/z 46. An example for a confirmatory analysis of phenylureas in a real sample has already been shown in Figure 3.

The amount of decomposition strongly depends on the temperature, both T_g and T_v. As shown by Cairns and Siegmund [25] for neburon, this fragmentation is probably due to a decomposition of the neutral ureas in the vaporizer probe prior to ionization. Surprisingly, of the two possible products formed by this decomposition process, predominantly one product is observed as an ionized species under our experimental conditions, viz. m/z 46. Whereas the relative abundance of the cationized isocyanates is low in each case and does

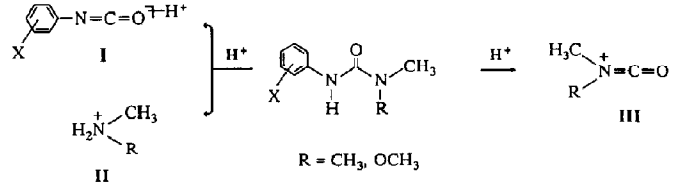

diuron:	I = m/z 188, 205, 222	II = m/z 46	III = m/z 72
monolinuron:	I = m/z 154, 171, 188	II = m/z 62	III = m/z 88

Scheme I

Table 5. Major ions observed for several phenylureas using various LC-MS ionization techniques[a]

Compound	Ionization	$[MH]^+/[M \cdot A]^+$[b]	$[PheNCO + H]^+/[PheNCO + A]^+$	$[H_2N(CH_3)R]^+$[c]	$[R(CH_3)NCO]^+$	Other ions
Chlorbromuron	APCI	293(100)	—	62(1)	88(2)	
$M_n = 292$	ESI	293(100)	—	—	88(5)	
	FAB	293(100)/315(10)	—	62(10)	88(5)	206(10)
	TSP[d]	293(100)/310(20)	232(3)	62(2)	—	215(15), 151(45)
Chlorotoluron	APCI	213(100)	—	46(1)	72(10)	148(5)
$M_n = 212$	ESI	213(100)	—	—	72(5)	
	FAB	213(100)	—	46(8)	72(40)	
	TSP	213(100)/230(5)	185(7)/202(5)	46(45)	—	179(5)
Difenoxuron	APCI	287(100)	—	46(1)	72(5)	123(5)
$M_n = 286$	ESI	287(100)	—	—	72(4)	
	FAB	287(100)/309(10)	—	—	72(22)	241(20), 123(15)
	TSP	287(100)	—	46(39)	—	216(40)
Diuron	APCI	233(100)	222(5)	46(3)	72(15)	278(10)
$M_n = 232$	ESI	233(100)/255(10)	—	—	72(12)	
	FAB	233(100)	—	46(5)	72(45)	386(8)
	TSP	233(100)	188(2)/205(5)/222(3)	46(50)	—	199(5)
Isoproturon	APCI	207(100)	—	46(3)	72(12)	
$M_n = 206$	ESI	207(100)	—	—	72(5)	
	FAB	207(100)/229(90)	—	46(15)	72(20)	191(20), 146(10)
	TSP	207(100)/224(5)	179(10)/196(2)	46(50)	—	252(4)
Linuron	APCI	249(100)/266(5)	—	62(2)	88(2)	
$M_n = 248$	ESI	249(100)	—	—	88(4)	
	FAB	249(100)/271(10)	—	62(10)	88(5)	
	TSP	249(100)/266(20)	205(5)	62(3)	88(1)	219(17)
Metobromuron	APCI	259(100)	—	—	88(4)	
$M_n = 258$	ESI	259(100)	—	—	—	
	FAB	259(100)/281(10)	—	62(8)	88(5)	
	TSP	259(100)/276(10)	215(3)	62(2)	—	229(5), 151(20)
Metoxuron	APCI	229(100)	—	46(3)	72(18)	
$M_n = 228$	ESI	229(100)/251(20)	—	—	72(5)	
	FAB	229(100)/251(10)	—	46(8)	72(50)	183(10)
	TSP	229(100)/246(5)	184(2)/201(10)/218(3)	46(35)	—	195(10), 185(5)
Monolinuron	APCI	215(100)/232(5)	—	62(2)	88(3)	126(10)
$M_n = 214$	ESI	215(100)/232(5)	—	—	88(3)	
	FAB	215(100)/237(15)	—	62(5)	88(5)	
	TSP	215(100)/232(10)	171(3)/188(2)	62(2)	—	185(5)
Monuron	APCI	199(100)	—	46(1)	72(20)	
$M_n = 198$	ESI	199(100)	—	—	72(5)	
	FAB	199(100)/221(40)	—	46(2)	72(55)	
	TSP	199(100)/216(4)	171(10)/188(5)	46(55)	—	

[a]The ion abundances (in parentheses) are expressed as a percentage of relative abundance. The experimental conditions are described in the Experimental section.
[b]Cluster ion $[M \cdot A]^+$; A = NH_4^+, $NH_3NH_4^+$, or Na^+
[c]R = $-CH_3$ or $-OCH_3$.
[d]Discharge-assisted buffer ionization.

not depend on T_v even at a very high vaporizer temperature (T_v = 250 °C). This is in contrast to the results of Cairns and Siegmund [25], who reported the abundant formation of cationized isocyanate. This divergence probably is due to the different design of the TSP interfaces. Further experiments with a Finnigan-MAT TSP source revealed a major abundance of the isocyanate in the TSP spectrum of diuron (m/z 205 and 222). Moreover, the ion abundance of diuron is strongly dependent on the vaporizer temperature with this source, indicating a decomposition prior to ionization (see Figure 7a for T_1' = 70 and 95 °C). Careful adjustment of the interface temperatures enables reproducible results and the thermally assisted degradation can be used to generate structurally specific ions in the TSP spectrum. An interlaboratory comparative study of several carbamates and phenylureas with respect to ion formation and sensitivity obtained with different TSP interfaces of several manufacturers has been conducted under well defined comparative experimental conditions. Results of this study are now under development and will be presented in a subsequent article.

So far, we have assumed that phenylureas undergo thermal decomposition of the neutral molecule to form the isocyanate and the corresponding amine, which are protonated in a second step. To confirm this assumption, additional CAD experiments were performed with

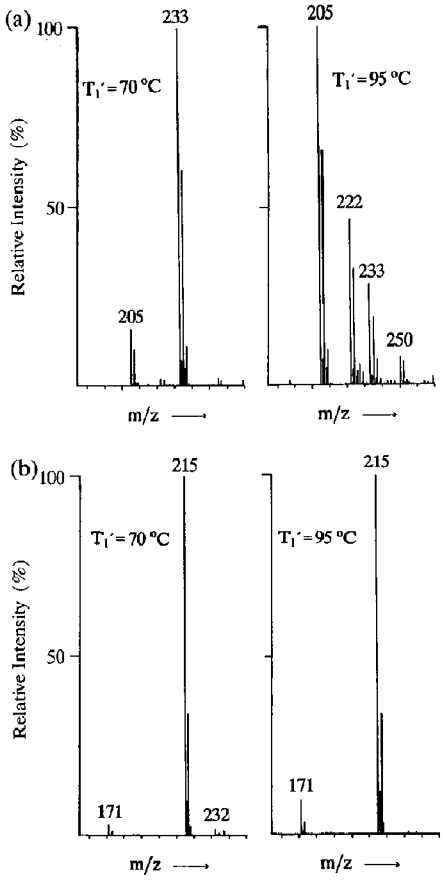

Figure 7. Thermal degradation of phenylureas to their isocyanates and variation of ion abundances in the TSP spectra of *N,N*-dimethylureas and *N*-methoxy-*N*-methylureas with vaporizer temperature. (**a**) Diuron and (**b**) monolinuron. Amount injected: 100 ng.

diuron and monolinuron. The results of these measurements are summarized in Table 6. CAD spectra of phenylureas already have been discussed by others [20, 25, 26]. However, the reported results are, in part, contradictory. Thus differences are observed as compared to the results of Niessen et al. [20], who only reported *m/z* 72 (III) in the TSP MS/MS spectrum of diuron, whereas Cairns and Siegmund [25] observed abundant protonated amine (II) (35% relative abundance) in the CAD spectra of neburon, and McFadden and Lammert [26] found *m/z* 46 (50%) and *m/z* 72 (100%) in TSP CAD experiments with difenoxuron and isoproturon. Our CAD results are in agreement with the latter, as can be seen from Table 6. The CAD spectra demonstrate, at least for diuron, that decomposition not only of the neutral molecule, but also the protonated molecule, may lead to the formation of **I** and **II** in the TSP source (apparently in the case of the Vestec source).

The TSP spectra of *N*-methyl-*N*-methoxy-phenylureas show only weak intensities of the corresponding amine at *m/z* 62 and of the isocyanate. Even an increase of T_v has only a slight effect on the fragment ion abundance (Figure 7b). Generally, *N*-methyl-*N*-methoxy-phenylureas are more stable and are even amenable to on-column injection GC analysis. Probably, the basicity of the *N,N*-dialkylated nitrogen atom is decreased by the additional oxygen atom in such a way that protonation most likely occurs at the phenyl-bound nitrogen of the urea function. Figure 8 demonstrates the stability of *N*-methoxy-*N*-methyl-phenylureas in comparison to their corresponding *N,N*-dimethyl-phenylureas. The figure shows a time-scheduled TSP SIM chromatogram of three *N*-methyl-*N*-methoxy-phenylureas (monolinuron, linuron, and chlorbromuron) and three *N,N*-dimethyl-phenylureas (fenuron, monuron, and diuron) under typical operating conditions ($T_g \approx 235$ °C and $T_v \approx 200$ °C). Although the latter compounds exhibit abundant ions of type II (*m/z* 46), the corresponding ion for *N*-methoxy-type phenylureas at *m/z* 62 is of very low abundance.

Ions corresponding to structure III at *m/z* 72 or 88 are missing in the discharge-assisted buffer ionization spectra, although the fragment at *m/z* 72 apparently has a low appearance energy [20].

OTHER IONIZATION TECHNIQUES. With ESI and FAB ionization, the fragmentation is reversed with respect to the structure: the ions at *m/z* 46 and 62 are less intensive or even absent whereas species III (Scheme I)

Table 6. Fragments obtained by collision-activated dissociation of ions in the TSP mass spectra of diuron and monolinuron[a]

Compound	Precursor ion		Daughter ions
	Tentative structure	*m/z*	*m/z* (% relative abundance)
Diuron	$[MH]^+$	233	188(3), 160(8), 72(100), 46(8)
	$[\text{isocyanate} \cdot H \cdot (NH_3)_2]^+$	222	205(53), 188(13), 162(100), 160(15), 127(85)
	$[\text{isocyanate} \cdot H \cdot NH_3]^+$	205	205(20), 188(15), 162(100), 160(10), 127(80)
Monolinuron	$[MH]^+$	215	183(5), 148(45), 146(10), 128(34), 126(100), 119(10), 99(20), 90(5), 62(10), 60(5)
	$[\text{isocyanate} \cdot H \cdot NH_3]^+$	171	171(3), 154(3), 128(40), 126(22), 111(2), 93(100)

[a] COFF = −20 V; collision cell pressure: argon, 1.3×10^{-3} torr.

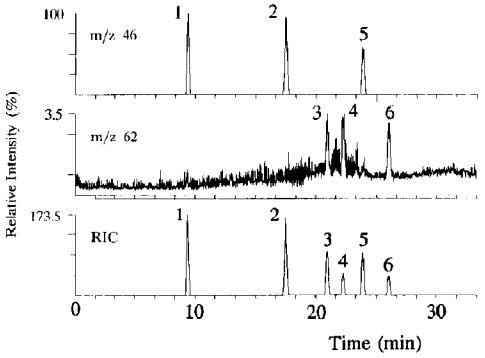

Figure 8. Discharge-assisted TSP SIM chromatogram of three *N,N*-dimethyl-phenylureas and three *N*-methoxy-*N*-methyl-phenylureas by simultaneously recording the $[MH]^+$ ions and their degradation products at m/z 46 and 62. Peak assignments: 1, fenuron; 2, monuron; 3, monolinuron; 4, diuron; 5, linuron; 6, chlorbromuron. Injected amount: 50 ng each.

is favored at least for the *N,N*-dimethylureas (Table 5). This behavior is expected because less thermal stress occurs during ionization via ESI and FAB as compared to TSP. Surprisingly, this behavior is also observed with APCI by using ammonium acetate by applying the same gradient and buffer conditions as described for TSP operation (see Experimental section). Although ionization conditions are very similar to thermospray, no intense ions at m/z 46 and 62 are observed with APCI in contrast to TSP ionization. However, when using ESI and APCI, confirmation of *N,N*-dimethyl-phenylureas during chromatographic analysis is quite possible by using the ion at m/z 72 (species **III**). In the case of the Finnigan-MAT APCI and ESI source, the intensity of this ion can be strongly enhanced for all investigated *N,N*-dimethyl-phenylureas if a collision offset is applied to the built-in octopole rods. For example, if 30 V are applied, the intensity of m/z 72 amounts to 70–95% of the total ion current.

Also under ESI and APCI conditions, *N*-methyl-*N*-methoxy-phenylureas are more stable and show only low fragmentation. That is, the ion at m/z 88 (species **III**) is only formed with low abundances (< 1%) similar to the ion m/z 62 in the TSP mode.

AMINE CLUSTERS. The postcolumn addition of alkylated amines in the TSP mode, as described in the previous section, was successfully applied to several carbamates and phenylureas (an example is shown in the following section). In general, most carbamates and phenylureas investigated exhibit the $[M \cdot H \cdot amine]^+$ ion instead of the protonated or ammonium-cationized molecule as base peaks because their proton affinities are lower than those of the amines (see previous section for details). In addition, phenylureas give POD reactions that enhance structural information. The dimethylated phenylureas undergo a carbonyl reaction, that is, the *N,N*-dimethyl group is in part replaced by the added aliphatic amine: $Phe{-}NH{-}CO{-}N(CH_3)_2 + H_2NC_nH_{2n+1} \rightarrow Phe{-}NH{-}CO{-}NHC_nH_{2n+1} + HN(CH_3)_2$. Thus $[M_s \cdot H \cdot amine]^+$ ions are formed in addition to the $[M \cdot H \cdot amine]^+$ ions, which represent the base peak in each case. For example, diuron ($M_n = 232$) exhibits these ions at m/z 306 (i-$C_3H_7NH_2$, 70% relative abundance), m/z 334 (t-$C_4H_9NH_2$, 3%), m/z 362 (n-$C_5H_{11}NH_2$, 45%), and m/z 390 (n-C_6H_{13}, 55%). The low reaction yield observed in the case of *tert*-butylamine is probably due to a steric hindrance.

Sulfonylureas. For the confirmation of sulfonylureas no special technique is necessary because these compounds usually exhibit a wide spectrum of intense fragments in the TSP mode, whereas the quasimolecular ion is of very low intensity or even absent [27]. This situation is most probably due to thermal degradation reactions in the vaporizer probe [21]. We have investigated eight sulfonylureas by various ionization techniques. All compounds exhibit thermal and mass spectrometric dissociation in the TSP mode. Generally, characteristic ions from both moieties of the sulfonylurea group $R^1SO_2NHC(O)NHR^2$ are visible, for example, $[R^1SO_2]^+$, $[R^1SO_2NH_2 + H]^+$, $[R^1SO_2NH_2 + NH_4]^+$, $[R^2NH_2 + H]^+$, $[R^2NCO + H]^+$, and $[R^2NCO + NH_4]^+$. For example, metsulfuron-methyl (nominal mass 381) exhibits these ions at m/z 199, 216, 233, 141, 167, and 184 in the TSP spectrum. No ions corresponding to the intact molecule were observed. As expected, the APCI spectrum (plus ammonium acetate) of metsulfuron-methyl is consistent with the TSP results, although an abundant protonated molecule at m/z 381 was additionally observed (70% relative abundance). The ESI and FAB spectra of metsulfuron-methyl exhibit only quasimolecular ions. In addition to the protonated molecule (ESI, 50%; FAB, 30%) both spectra show abundant sodium-cationized ions at m/z 404 (= $[M + Na]^+$; ESI, 100%; FAB, 55%) and 426 (= $[M - H + 2Na]^+$; ESI, 15%; FAB, 100%).

An example of the combined on-line trace enrichment and TSP LC-MS analysis of sulfonylureas in aqueous samples is shown in Figure 9. More details concerning the on-line solid-phase extraction technique are reported elsewhere [28].

Amines, anilides, and organophosphorous compounds

FRAGMENTATION. The TSP mass spectra of most of the investigated anilides and *N*-substituted amines (Table 1) contain significantly more fragmentation than those of the phenylureas and triazines. This is demonstrated in Figure 10a, where the discharge-assisted buffer ionization spectrum of the anilide butachlor is shown. The relative abundance in the TSP spectra of

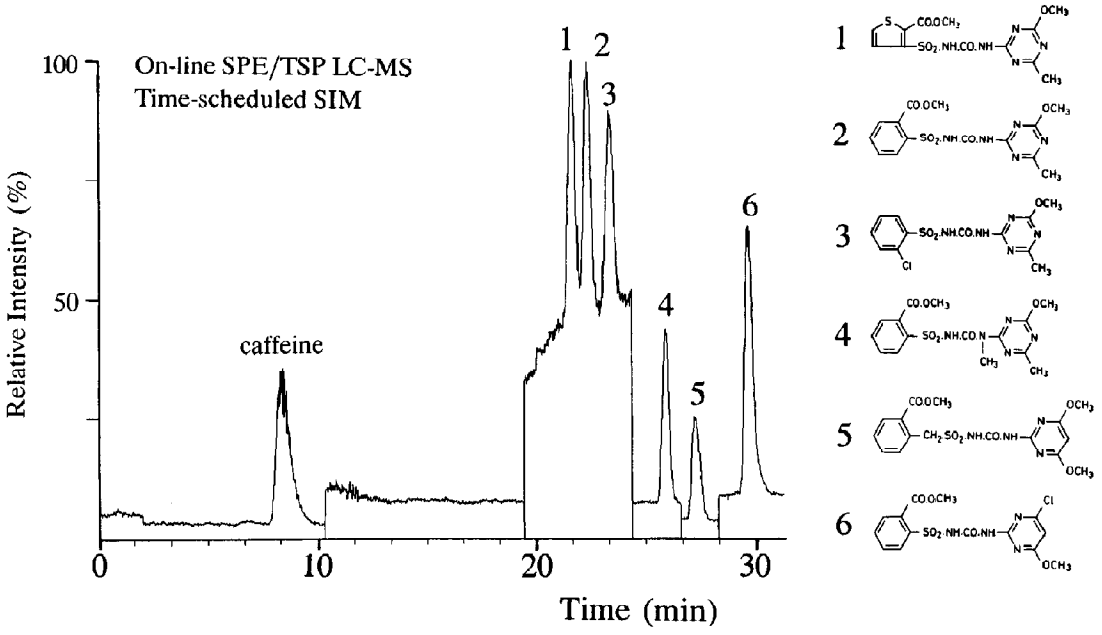

Figure 9. On-line trace enrichment TSP LC-MS traces for 100 mL of a drinking water sample spiked with a mixture of six sulfonylureas at 150 ng/100 mL. Time-scheduled SIM traces of the $R^2NH_3^+$ ions formed from the dissociation of the sulfonylureas (the intensity of these $R^2NH_3^+$ ions amount to 60–90% of the TIC; R^2 = *N*-heterocyclic moiety). Peak assignments: 1, thifensulfuron-methyl; 2, metsulfuron-methyl; 3, chlorsulfuron; 4, tribenuron-methyl; 5, bensulfuron-methyl; 6, chlorimuron-methyl.

butachlor and other anilides varies greatly with interface temperatures, as previously reported by us [7] for alachlor, especially for chloroacetic acid *N*-alkoxymethylanilides, (e.g., alachlor and butachlor).

Such observations can be rationalized in terms of "chemical dissociation," where the analyte molecule degrades prior to ionization, probably induced by buffer salt, heat, or solvent followed by ionization of the degradation products, sometimes with successive fragmentations. This scenario is especially valid for alachlor and butachlor, where the discharge-assisted buffer ionization spectra mainly exhibit quasimolecular ions, that is, $[MH]^+$ and $[MH \cdot NH_3]^+$ (m/z 270, 287, and 312, 329, respectively) for $T_g < 200$ °C, whereas for $T_g > 250$ °C the base peak at m/z 226 is due to a thermolysis reaction prior to ionization (Scheme II). These particular ions do not occur in the corresponding FAB and ^{252}Cf plasma desorption spectra, nor do they appear in the electrospray or CAD spectra (Figure 10b–d). The product ion spectrum of the precursor ion m/z 312 exhibits the ions at m/z 238 and 162. The ESI tandem mass spectrometry spectra of alachlor, dimethachlor, and metolachlor follow the same fragmentation mechanisms. (The corresponding ions are explained in the following text.) The described temperature dependence readily can be used for confirmation purposes.

Not all abundant ions in the TSP spectra are due to a thermal degradation of the neutral molecule followed by ionization. Comparison of the FAB, ESI, ^{252}Cf-PD, and, in particular, the CAD spectrum of the quasimolecular ion reveals that the protonated molecule also degrades to give abundant fragments. Thus initial protonation at the ether oxygen atom with neutral loss of alcohol produces resonance-stabilized carbenium–imminium ions [alachlor and butachlor: m/z 238 (see Scheme II); dimethachlor: m/z 224; metolachlor: m/z 252 and 238 (loss of dimethylether)]. In a second step, these ions probably undergo further loss of neutral ketene to give a second carbenium–imminium ion in the FAB, TSP, and ^{252}Cf-PD as well as in the CAD spectra of the $[MH]^+$ ion (ESI MS/MS: m/z 162 for alachlor and butachlor; refer to Scheme II; m/z 148 for dimethachlor and m/z 176 for metolachlor), whereas this fragmentation is not observed in the ESI spectra. Smaller alkyl substituents between the nitrogen and the ether oxygen atom seem to enhance the primary fragmentation from the molecular ion: whereas fragments from the molecular ion corresponding to the loss of alcohol are absent in the TSP spectra of dimethachlor and metolachlor, they are also less intense in the corresponding ESI, FAB, and ^{252}Cf-PD spectra (Table 7). The formation of the secondary and tertiary carbenium–imminium ions is probably not fa-

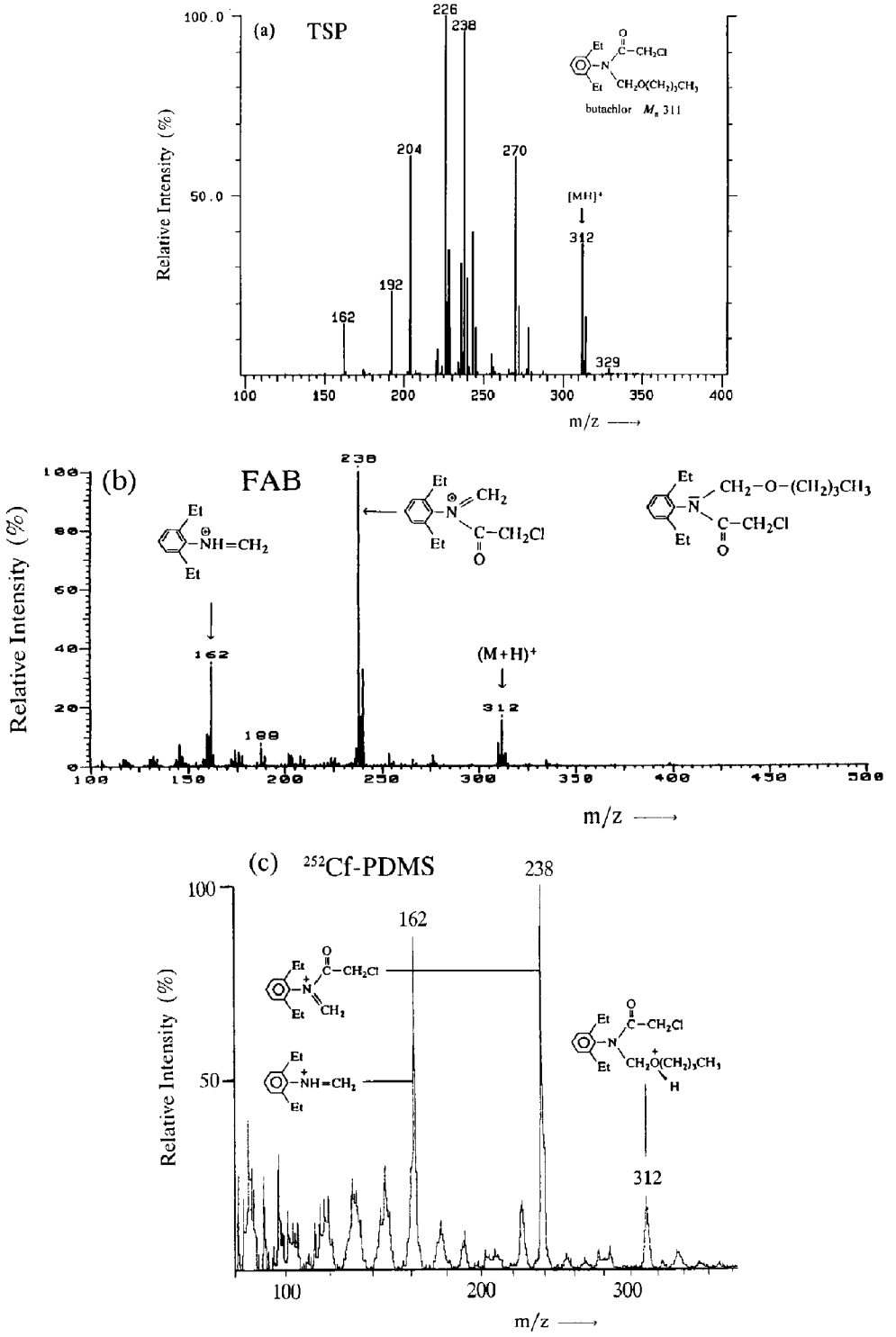

Figure 10. Mass spectra of butachlor obtained by various ionization techniques: (a) discharge-assisted thermospray (for peak assignment, refer to Scheme 2); (b) fast-atom-bombardment; (c) ^{252}Cf plasma desorption; (d) electrospray; (e) collision-activated dissociation.

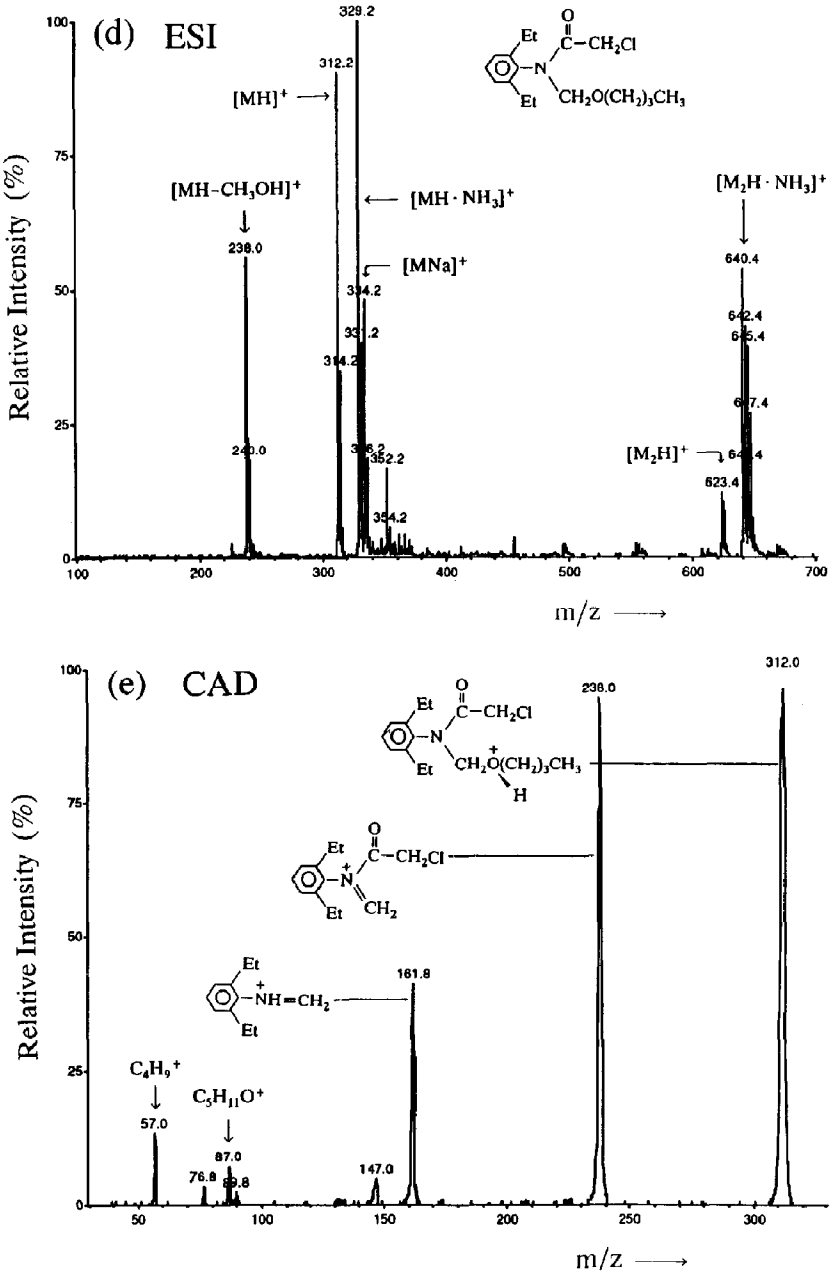

Figure 10. *(Continued)*

vored because an additional 1,2-hydrid shift is necessary.

This mechanism is also operative for structurally different anilides. For example, the TSP spectra of metazachlor exhibit an ion at m/z 210 that is probably due to a neutral loss of pyrazole after protonation at $N - 1$ of the pyrazole moiety.

DECHLORINATION. The intense peak at m/z 204 with no chlorine isotope pattern in the discharge-assisted buffer ionization spectra of butachlor (Figure 10a) probably corresponds to a chlorine–hydrogen substitution (Scheme II). Generally, the discharge-assisted buffer ionization and solvent-mediated CI spectra of all investigated anilides exhibit characteristic

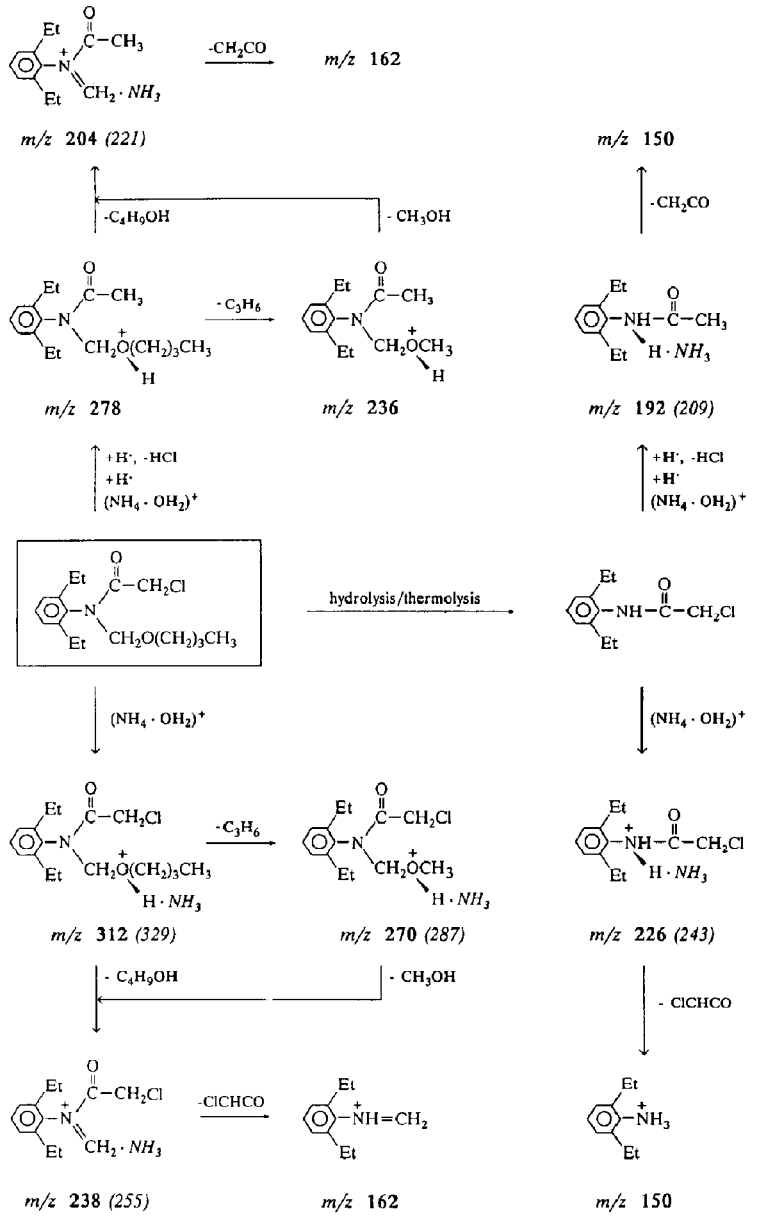

Scheme II

$[MH - 34]^+$ and [fragment $- 34]^+$ ions for all chlorine-containing species (see Figure 10a and Table 7). This substitution reaction is not observed in the buffer ionization mode [7] or via ESI, FAB, and ^{252}Cf-PD ionization. This reaction probably is due to a reductive dehalogenation involving replacement of a halogen atom by a hydrogen atom. The reaction also occurs with other compound classes such as chlorotriazines and phenylureas as already shown in Figures 4 and 5. As an example, the comparison of discharge-assisted buffer ionization and TSP mode is demonstrated in Figure 11, where the spectra of diuron are shown with either discharge-on or discharge-off operation but otherwise identical experimental conditions.

Generally, the amount of dechlorination is higher for aliphatic-bound chlorines, for example, higher for chloroanilides (dechlorination ranges from 10 to 50%) than for chlorine atoms bound to an aromatic ring (1–10%). These reductive dehalogenations probably take place via a radical reaction prior to ionization [29, 30] induced by radicals that are formed from the plasma generated in a CI source (refer to Figure 11).

Table 7. Major ions observed for chloroacetic acid *N*-alkoxy-methylanilides using various LC-MS ionization techniques[a]

Compound	Ionization	$[MH]^+/[M \cdot A]^+$[b]	$[M - X + 2H]^+$	$[MH - ROH]^+$	Other ions
Alachlor	ESI	270(85)/287(100)	—	238(70)	556(25)
$M_n = 269$	FAB	270(28)/—	—	238(100)	188(10), 162(30)
	TSP[c]	270(100)/287(6)	236(33)	238(77)	243(28), 226(88), 204(37), 192(10), 162(10), 150(5)
	^{252}Cf-PD	270(30)/—	—	238(95)	162(100)
	CAD[d]	270(100)	—	238(80)	162(68), 147(10), 45(15)
Butachlor	ESI	312(90)/329(100)/334(47)	—	238(60)	645(25), 640(50), 623(12)
$M_n = 311$	FAB	312(18)/334(3)	—	238(100)	162(45)
	TSP	312(37)/329(3)	278(15)	238(95)	287(12), 270(63), 243(40), 226(100), 204(60), 162(10)
	^{252}Cf-PD	312(13)/—	—	238(100)	162(65)
	CAD	312(100)	—	238(98)	162(45), 87(8), 57(12)
Dimethachlor	ESI	256(100)/273/(55)/278(22)	—	224(4)	528(55), 511(20)
$M_n = 255$	FAB	256(100)/278(40)	—	224(54)	197(15), 148(11), 59(8)
	TSP	256(100)/—	222(38)	—	—
	^{252}Cf-PD	256(100)/—	—	224(60)	148(34), 132(50)
	CAD	256(100)	—	224(67)	148(28), 132(5), 105(5), 77(5)
Metolachlor	ESI	284(100)/301(45)	—	252(2)	—
$M_n = 283$	FAB	284(100)/306(23)	—	252(68)	238(30), 206(10), 176(13), 162(28), 122(18), 73(30)
	TSP	284(100)/—	250(33)	—	—
	^{252}Cf-PD	284(75)/—	—	252(40)	238(100), 162(50)
	CAD	284(98)	—	252(100)	212(10), 176(25), 73(11)

[a]The ion abundances (in parentheses) are expressed as a percentage of relative abundance. The experimental conditions are described in the Experimental section.
[b]Cluster ion $[M \cdot A]^+$; $A = NH_4^+$ or Na^+.
[c]Discharge-assisted buffer ionization. In the buffer ionization mode no $[M - X + 2H]^+$ ions are observed! (See text.)
[d]Precursor ions $[MH]^+$ are generated by ESI tandem mass spectrometry; amount injected: 6 ng. For experimental conditions, refer to Table 5.

In the case of disubstituted and trisubstituted compounds, for example, for the trichlorinated aliphatic organophosphorous pesticides butonate and trichlorfon and the dichlorinated pesticide dichlorovos, all chlorine atoms are replaced successively under discharge-assisted buffer ionization (the spectra are not shown in this report), that is, $[M - xCl + (x + 1)H]^+$ ions ($x = 1$, 2, and 3) are observed with relative abundances of up to 50%, whereas in the TSP mode, again, no reductive dechlorination was observed [7].

It is interesting that in the case of anilazine, which contains three chlorines, abundant signals corresponding to dechlorination are observed only for two chlorines in the discharge-assisted TSP spectra, whereas the $[M_s - 3Cl + 4H]^+$ (M_s substitution product obtained by POD) ion abundance is very low. Apparently, both chlorines that are bound to the *N*-heterocyclic moiety are replaced favorably (Figure 5). However, diuron exhibits replacement of both phenyl-bound halogen atoms (Figure 11).

This behavior corresponds to findings of other authors, who report dehalogenations under CI conditions, for example, dechlorination reactions in the case of phenylureas [20]. Dehalogenations also reportedly occur as FAB-induced substitutions in the condensed phase via a free radical mechanism that precedes the ionization process, for example, with nucleosides [31, 32] and antibiotics [33]. Similar dehalogenations also are observed during ^{252}Cf plasma desorption and FAB ionization of 5-halouracils and thyroxine [34].

Conclusions

The purpose of the present work was to evaluate methods used for determination and confirmation of nitrogen- and phosphorus-containing pesticides by TSP LC-MS. After solid-phase extraction of aqueous water samples, pesticide residues readily can be identified, confirmed, and quantified at a concentration level of < 100 ng L^{-1} (which corresponds to the CEC drinking water limit). This level is achieved using gradient elution LC with time-scheduled SIM detection.

It has been shown that, through the combined use of several experimental parameters, both cationized molecules for molecular weight information and abundant fragment ions for structural confirmation from the TSP spectra can be obtained for the majority of the investigated pesticides. These parameters include a variation of the source and vaporizer temperature to induce thermal degradation and the use of different organic modifiers added postcolumn to the mobile phase. Thus, postcolumn on-line derivatization (POD) was achieved by adding different alkylated amines with varying proton affinities and nucleophilicities. In the case of chlorotriazines and several other *N*-heterocyclic compounds, this on-line derivatization led to chlorine substitution and amine adduct ion formation. Both processes can be used to enhance structural information and thus the specificity of the method. It is demonstrated for carbamates, phenylureas, and *N*-heterocyclic compounds that the proton affinity has a

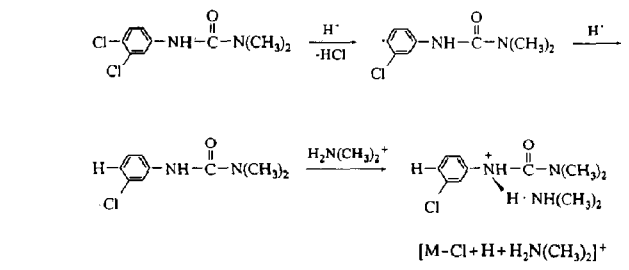

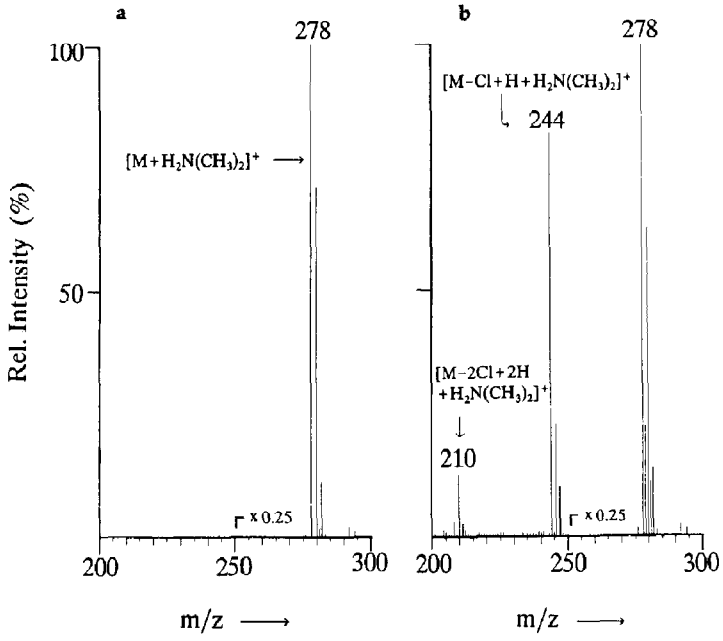

Figure 11. Comparison of ionization modes in the TSP analysis of diuron after POD with dimethylamine and proposed fragmentation pathway. (a) Buffer ionization (discharge-off) and (b) solvent-mediated CI (discharge). Amount injected: 500 ng.

strong influence on the ion abundance in the TSP spectra.

It has been demonstrated that the combination of different mass spectrometry ionization techniques such as APCI, CAD, ^{252}Cf-PD, ESI, FAB, and TSP is useful for the elucidation of fragmentation mechanisms in TSP mass spectra. These techniques were applied to the analysis of phenylureas and anilides. The fragmentation and degradation reactions studied include reductive dehalogenations, nucleophilic substitutions, and thermal decompositions. The information obtained from this comparative study should facilitate the identification, quantification, and confirmation of pesticide residues in complex aqueous matrices by TSP LC-MS.

Acknowledgments

Grateful acknowledgment is made to Dr. Hans-Martin Schiebel from the mass spectrometric facility of the Technische Universität Braunschweig, Germany, where the FAB studies were carried out. We are also grateful to Dr. Wolfgang Dreher (BASF AG, Limburgerhof, Germany) and Dr. Winfried Wagner-Redeker (Finnigan MAT, Bremen, Germany) for technical support during APCI and ESI experiments, to Dr. Manfred Raida (Institut für Peptidforschung, Hannover, Germany) for the ^{252}Cf-PDMS experiments and to Sylvia Kramer and Dr. Jochen Schmidt (Solvay Deutschland, Hannover, Germany) for the comparative experiments with the Finnigan MAT TSP source. The authors wish to thank Ference Toth for his assistance during on-line enrichment experiments. This research was supported by funds from the Bundesministerium für Forschung und Technologie (Bonn, Germany).

References

1. U.S. Environmental Protection Agency, National Survey of Pesticides in Drinking Water Wells, Phase I Report: 1990; Office of Water and Office of Pesticides Programs, U.S. Government Printing Office: Washington, DC, 1990; EPA-570/9-90-015.
2. Commission of the European Communities, EEC Drinking Water Guideline; 80/779/EEC, EEC No. L229/11-29; EEC: Brussels, August 30th, 1980.

3. Böhm, H. B.; Feltes, J.; Volmer, D.; Levsen, K. *J. Chromatogr.* **1989**, *478*, 399–407.
4. De Kok, A.; Hiemstra, M.; Brinkman, U. A. Th. *J. Chromatogr.* **1992**, *623*, 265–276.
5. Bellar, T. A.; Budde, W. L. *Anal. Chem.* **1988**, *60*, 2076–2083.
6. Volmer, D.; Levsen, K.; Wünsch, G. *J. Chromatogr.*, **1994**, *660*, 231–248.
7. Volmer, D.; Preiss, A.; Levsen, K.; Wünsch, G. *J. Chromatogr.* **1993**, *647*, 235–259.
8. Barceló, D. *Biomed. Environ. Mass Spectrom.* **1988**, *17*, 363–369.
9. Farran, A.; De Pablo, J.; Barceló, D. *J. Chromatogr.* **1988**, *455*, 163–172.
10. Barceló, D. *Org. Mass Spectrom.* **1989**, *24*, 219–224.
11. Voyksner, R. D. In *Applications of New Mass Spectrometry Techniques in Pesticide Chemistry;* Rosen, J. D., Ed.; Wiley: New York, 1987; p 146.
12. Jones, T. L.; Betowsky, L. D.; Yinon, J. In *Liquid Chromatography/Mass Spectrometry. Applications in Agricultural, Pharmaceutical, and Environmental Chemistry;* Brown, M. A., Ed.; ACS Symposium Series 420; American Chemical Society: Washington, DC, 1990, p 62.
13. Voyksner, R. D.; McFadden, W. H.; Lammert, S. A. In *Applications of New Mass Spectrometry Techniques in Pesticide Chemistry;* Rosen, J. D., Ed.; Wiley: New York, 1987; p 247.
14. Barceló, D.; Durand, G.; Vreeken, R. J.; De Jong, G. J.; Lingeman, H.; Brinkman, U. A. Th. *J. Chromatogr.* **1991**, *553*, 311–328.
15. Vreeken, R. J.; Van Dongen, W. D.; Ghijsen, R. T.; Brinkman, U. A. Th. *Int. J. Environ. Anal. Chem.*, **1994**, *54*, 119–145.
16. Behymer, T. D.; Bellar, T. A.; Budde, W. L. *Anal. Chem.* **1990**, *62*, 1686–1690.
17. Pleasance, S.; Anacleto, J. F.; Baily, M. R.; North, D. H. *J. Am. Soc. Mass Spectrom.* **1992**, *3*, 378–397.
18. Lin, H.; Voyksner, R. D. *Anal. Chem.* **1993**, *65*, 451–456.
19. Chiu, K. S.; Van Langenhove, A.; Tanaka, C. *Biomed. Environ. Mass Spectrom.* **1989**, *18*, 200–206.
20. Niessen, W. M. A.; Van der Hoeven, R. A. M.; De Kraa, M. A. G.; Herremans, C. E. M.; Tjaden, U. R.; Van der Greef, J. *J. Chromatogr.* **1989**, *478*, 325–338.
21. Niessen, W. M. A.; Van der Greef, J. *Liquid Chromatography–Mass Spectrometry. Principles and Applications;* Marcel Dekker: New York, 1992; p 403.
22. Lias, S. G.; Bartness, J. E.; Liebman, J. F.; Holmes, J. L.; Levin, R. D.; Mallard, W. G. *J. Phys. Chem. Ref. Data* **1988**, *17*(suppl 1), 23.
23. Hartman, K. N.; Lias, S.; Ausloos, P.; Rosenstock, H. M.; Schroyer, S. S.; Schmidt, C.; Martinsen, D.; Milne, G. W. A. A Compendium of Gas Phase Basicity and Proton Affinity Measurements; NBSIR 79-1777; National Bureau of Standards: Washington, DC, 1979.
24. Tamiri, T.; Zitrin, S. *Biomed. Environm. Mass Spectrom.* **1987**, *14*, 39–46.
25. Cairns, T.; Siegmund, E. G. In *Liquid Chromatography/Mass Spectrometry. Applications in Agricultural, Pharmaceutical, and Environmental Chemistry;* Brown, M. A., Ed.; ACS Symposium Series 420; American Chemical Society: Washington, DC, 1990, p 40.
26. McFadden, W. H.; Lammert, S. A. *J. Chromatogr.* **1987**, *385*, 201–211.
27. Shalaby, L. M.; Bramble, F. Q.; Lee, P. W. *J. Agric. Food Chem.* **1992**, *40*, 513–517.
28. Volmer, D.; Levsen, K.; Engewald, W. *Vom Wasser*, **1994**, *82*, 335–364.
29. Madhusudanan, K. P.; Murthy, V. S. *J. Chem. Soc. Perkin Trans. 2* **1989**, *9*, 1255–1260.
30. Budzikiewicz, H. *Org. Mass. Spectrom.* **1988**, *23*, 561–565.
31. Schiebell, H.-M.; Schulze, P.; Leibfritz, D.; Jastorf, B.; Maurer, K. H. *Biomed. Mass Spectrom.* **1985**, *12*, 170–180.
32. Musser, S. M.; Kelley, J. A. *Org. Mass Spectrom.* **1993**, *28*, 672–678.
33. Siegel, M. M.; McGahren, W. J.; Ellestad, G. A. In *Mass Spectrometry in the Analysis of Large Molecules;* McNeal, C. J., Ed.; Wiley: New York, 1986; p 207.
34. Yang, Y.-M.; Fales, H. M.; Pannell, L. *Anal. Chem.* **1985**, *57*, 1771–1772.